



Molecular Crystals and Liquid Crystals Science and Technology. Section A. Molecular Crystals and Liquid Crystals

Publication details, including instructions for authors and
subscription information:

<http://www.tandfonline.com/loi/gmcl19>

Organic/Inorganic Molecular Beam Epitaxy (O/I-MBE): Formation and Characterization of Ordered Phthalocyanine Thin Films - Photoelectrochemical Processes

L.-K. Chau^a, S.-Y. Chen^a, N. R. Armstrong^a, G. E. Collins^a,
C. D. England^a, V. S. Williams^a, M. L. Anderson^a, T. J.
Schuerlein^a, P. A. Lee^a, K. W. Nebesny^a, B.A. Parkinson^b &
C. Arbour^c

^a Department of Chemistry, University of Arizona, Tucson,
Arizona, 85721

^b Department of Chemistry, Colorado State University, Fort
Collins, Colorado, 80523

^c Research Center for Photobiophysics, University of Quebec,
Trois-Rivier, Canada

Version of record first published: 24 Sep 2006.

To cite this article: L.-K. Chau, S.-Y. Chen, N. R. Armstrong, G. E. Collins, C. D. England, V. S. Williams, M. L. Anderson, T. J. Schuerlein, P. A. Lee, K. W. Nebesny, B.A. Parkinson & C. Arbour (1994): Organic/Inorganic Molecular Beam Epitaxy (O/I-MBE): Formation and Characterization of Ordered Phthalocyanine Thin Films - Photoelectrochemical Processes, *Molecular Crystals and Liquid Crystals Science and Technology. Section A. Molecular Crystals and Liquid Crystals*, 252:1, 67-77

To link to this article: <http://dx.doi.org/10.1080/10587259408038212>

PLEASE SCROLL DOWN FOR ARTICLE

Full terms and conditions of use: <http://www.tandfonline.com/page/terms-and-conditions>

This article may be used for research, teaching, and private study purposes. Any substantial or systematic reproduction, redistribution, reselling, loan, sub-licensing, systematic supply, or distribution in any form to anyone is expressly forbidden.

The publisher does not give any warranty express or implied or make any representation that the contents will be complete or accurate or up to date. The accuracy of any instructions, formulae, and drug doses should be independently verified with primary sources. The publisher shall not be liable for any loss, actions, claims, proceedings, demand, or costs or damages whatsoever or howsoever caused arising directly or indirectly in connection with or arising out of the use of this material.

ORGANIC/INORGANIC MOLECULAR BEAM EPITAXY (O/I-MBE): FORMATION AND CHARACTERIZATION OF ORDERED PHthalOCYANINE THIN FILMS -- PHOTOELECTROCHEMICAL PROCESSES

L.-K. Chau, S.-Y. Chen, **N.R. Armstrong***, G.E. Collins, C.D. England,
V.S. Williams, M.L. Anderson, T.J. Schuerlein, P.A. Lee, K.W. Nebesny,
Department of Chemistry, University of Arizona, Tucson, Arizona 85721;
B.A. Parkinson, Department of Chemistry, Colorado State University, Fort
Collins, Colorado 80523, and C. Arbour, Research Center for
Photobiophysics, University of Quebec, Trois-Rivier, Canada.

Abstract -- Photoelectrochemical processes are described for epitaxial phthalocyanine thin films on SnS_2 single crystal photoelectrodes. Square lattice formation is indicated during the nucleation of the ordered monolayers of the trivalent metal Pc's (e.g. InPc-Cl) and the tetravalent metal Pc's (e.g. VOPc). Multilayer growth leads to packing structures which strongly red-shift (VOPc , InPc-Cl) or blue-shift (AlPc-F) the Q-band photocurrent spectra, in accordance with established models for exciton coupling effects. Quantum yields for photocurrent production versus Pc coverage are consistent with the requirement for exciton diffusion from the point of excitation in the Pc multilayer to the SnS_2 interface, where charge injection occurs.

Keywords: photoelectrochemistry, epitaxial, phthalocyanine, multilayers, exciton coupling, ultrathin films, metal dichalcogenides

Introduction

Large aromatic dyes such as phthalocyanines exhibit epitaxial growth during vacuum deposition as ultrathin films, provided that a "layer-by layer" growth mode can be sustained (substrate temperatures above 100°C , with coverages extending up to several tens of monolayers.¹⁻¹⁵ Deposition of these dye films by a molecular beam epitaxy process allows for closer packing of the highly ordered chromophores than in self-assembled (SA) or Langmuir-Blodgett (LB) thin films, owing to the lack of hydrocarbon side chains necessary for control of molecular architecture during LB or SA deposition. Phthalocyanines with trivalent or tetravalent metal centers (e.g. InPc-Cl , GaPc-Cl , AlPc-Cl , AlPc-F and VOPc) have demonstrated epitaxial growth to form commensurate or coincident lattices (as confirmed by surface electron diffraction), along with a few modified perylene dyes.¹⁻¹¹ Substrates of particular interest to us for organic-MBE have been the metal dichalcogenides such as SnS_2 , and MoS_2 . These materials are available as freshly cleaved single crystals, however SnS_2 substrates can also be grown by a molecular beam epitaxy process on optically transparent substrates such as mica.⁴ The bandgap of SnS_2 ($E_{\text{BG}} = 2.2 \text{ eV}$) makes optical characterization of the resultant thin film dye assembly straightforward.

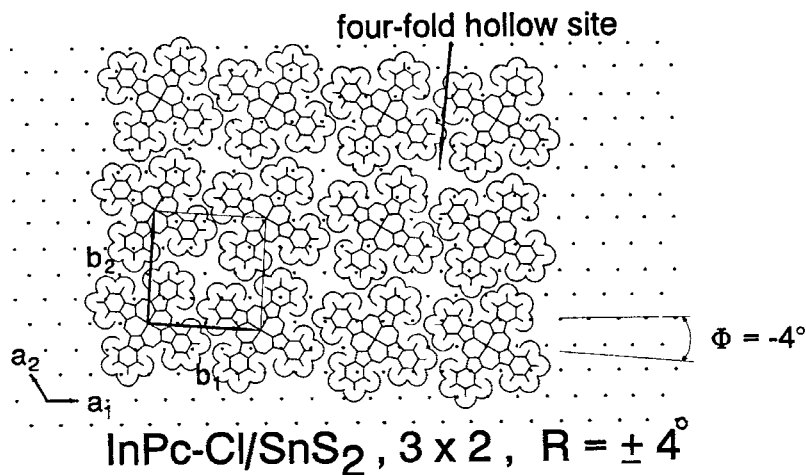
These metal dichalcogenides possess basal plane surfaces which interact weakly with most overlayers. Initial assumptions were made, therefore, that intermolecular forces primarily govern the packing of molecular crystals in the first monolayer.¹⁷ Nucleation may occur at defect sites on the basal plane of these substrates, but these defects do not appear to dictate the orientation of the resulting epitaxial layers. Modeling studies of epitaxial monolayers, whose size exceeds ca. 6-9 molecules, demonstrate that the orientation of the assembly, with respect to the major azimuthal axes of the substrate, may be dictated by the accumulation of van der Waals forces between substrate and overlayer.¹⁸ Epitaxial layers of Pc's and perylenes, obtained on cleaved single crystals of salts such as KCl and KBr, appear to be subject to additional electrostatic forces, which combine with van der Waals interactions to dictate the orientation and structure of the organic overlayers.⁵⁻¹⁶

Doped single crystal SnS_2 acts as a unique photoelectrode -- dyes adsorbed at low coverage on the SnS_2 surface, in contact with transparent aqueous electrolytes, inject charge into the conduction band of the substrate semiconductor, and produce photocurrents which allow for the spectroscopic characterization of the dye overlayer, at submonolayer sensitivities.¹⁹ Epitaxial layers of the chloroindium phthalocyanine (InPc-Cl) show high quantum yields per absorbed photon (QYAP up to ca. 50%), and photocurrent spectra which correlate well with the degree of ordering demonstrated from surface electron diffraction data.² These earlier studies now include other trivalent metal Pc's (AlPc-Cl, AlPc-F, GaPc-Cl) and the tetravalent metal Pc, vanadyl phthalocyanine (VOPc), all of which exhibit epitaxy as thin films.

The dye-sensitized photocurrent, J , is proportional to the absorbed light intensity, $J = \phi I_0(1 - e^{-\beta t})$, where ϕ is the quantum yield of carrier generation, I_0 is the incident light intensity, β is the absorption coefficient of the film, and t is the dye layer thickness.²⁰⁻²⁴ The photocurrent spectrum can coincide with the absorption spectrum if βt is small and the quantum yield for photoinjected charge is independent of wavelength (i.e. all absorbed photons produce excited states with equal probability of charge injection, see below). Under these conditions, $J \approx \phi I_0 A$, where A is the absorbance of the film, and the action spectrum of the sensitized photocurrent will correspond to the absorption spectrum. For light absorbed in multilayer dye films, energy must migrate to the SnS_2 interface through exciton diffusion.²⁵ It is believed that only those excitons which are absorbed at, or transported to, the semiconductor electrode surface layer will be active in producing photocurrent.²⁰

Epitaxial Trivalent and Tetravalent Metal Phthalocyanine Monolayers

The structure determined for the first ordered monolayer of InPc-Cl, GaPc-Cl, AlPc-Cl and VOPc on SnS_2 are shown in Figure 1. The Pc's nucleate in square lattice configurations, with the flat-lying molecules spaced at ca. 13.7\AA . The major axis of each Pc square lattice is aligned along (MoS_2) or near ($\pm 4^\circ$ for SnS_2) the three principle axes of the substrate, leading to three equivalent domains for deposition on MoS_2 or six equivalent domains for deposition on SnS_2 .^{1,3} Square

Figure 1 -- Pc Square Lattice/ SnS_2

lattice packing is also observed for the first monolayer of VOPc on single crystal KBr, where the four-fold symmetry and unit cell parameters of the substrate allow for a uniaxial, single domain Pc monolayer to be formed.^{7,10} As discussed below

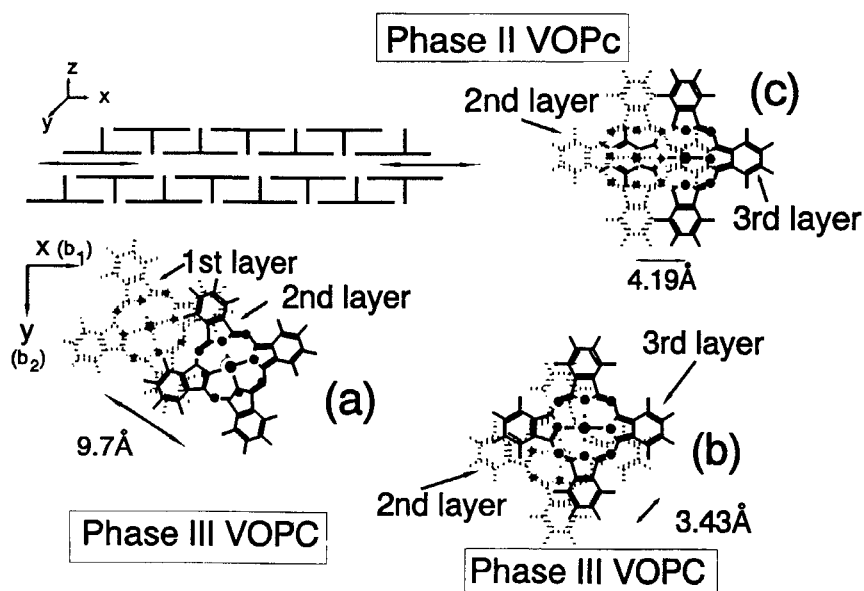


Figure 2 -- VOPc Ultrathin Films

the optical properties of these square lattice Pc films are similar, whether grown on the halide salts or the metal dichalcogenides.

Intersection of equivalent domains initiates second layer growth, in packing reminiscent of bulk structures known for the trivalent and tetravalent metal Pc's.²⁷⁻³⁴ "Layer-by-layer" growth conditions are sustainable for the trivalent metal Pc's, leading to reflection high energy electron diffraction (RHEED) data which are unchanged from that observed during formation of the first monolayer. The P1 space group packing structures of multilayers of epitaxially deposited trivalent metal (chloride) Pc's have been described previously.¹⁻⁴ The tendency toward polymorphism in VOPc leads to at least three structures on the SnS_2 surface, distinguishable by their absorbance or photocurrent spectra.³⁰⁻³² Figure 2 gives an overview of the structures possible for the second and subsequent monolayers of VOPc, and are derived from known or presumed bulk structures of VOPc.

Following formation of a square lattice monolayer (e.g. Figure 1, $\text{V}=\text{O}$ up), a second layer can form with the $\text{V}=\text{O}$ cation pointed toward the first layer, and with each Pc ring in the second layer shifted by 6.85\AA in the x direction and 6.85\AA in the y direction with respect to the Pc's in the first layer (Figure 2a). When the third layer is shifted as shown in Figure 2b, the resultant A/B/A'/B' packing leads to "Phase III" VOPc.³⁰ An alternate shift in the third layer Pc's produces the packing structure of "Phase II" VOPc (Figure 2c).³⁰ The exciton splitting produced by coupling of the transition dipoles in these structures, and the resultant photocurrent spectral shifts, are discussed below.

Dye Sensitization of SnS_2 Photoelectrodes: Photocurrent Action Spectra

Figure 3 shows the photocurrent action spectra for low coverages of InPc-Cl, VOPc and AlPc-F. InPc-Cl (Figure 3a) was deposited under conditions where the RHEED data suggested growth of flat-lying submonolayer domains, and onset of aggregation into second layers occurred prior to completion of the first equivalent monolayer. Without aggregation the Q-band spectrum peaks at 705 nm, and remains nearly as narrow as the solution absorbance spectrum.¹⁻⁴ The staggered geometry adopted by the second and subsequent layers (similar to that shown in Figures 2a and 2b) is made apparent by the striking red shift in the Q-band spectrum as coverage increases. The Q-band remains relatively narrow, with a FWHM less than 80 nm, consistent with the homogeneous packing environment for these epitaxial layers. Increasing coverages up to ca. 10ML show the Q-band maximum converging on a final value of 760 nm.¹⁻⁴ Once "layer-by-layer" growth modes are lost in the InPc-Cl/ SnS_2 system, these spectra broaden substantially in the wavelength region from 500-900 nm.

VOPc has shown a greater tendency toward the formation of aggregates when deposited on SnS_2 surfaces -- layered growth is more difficult to sustain above monolayer coverages than for the trivalent metal chloride Pc's. At the lowest coverages the Q-band spectrum (Figure 3b) is red-shifted by an amount consistent with the square lattice packing of the first monolayer segments of VOPc. Coverages equivalent to monolayer (Figure 3b) yield a red shift in the Q-band

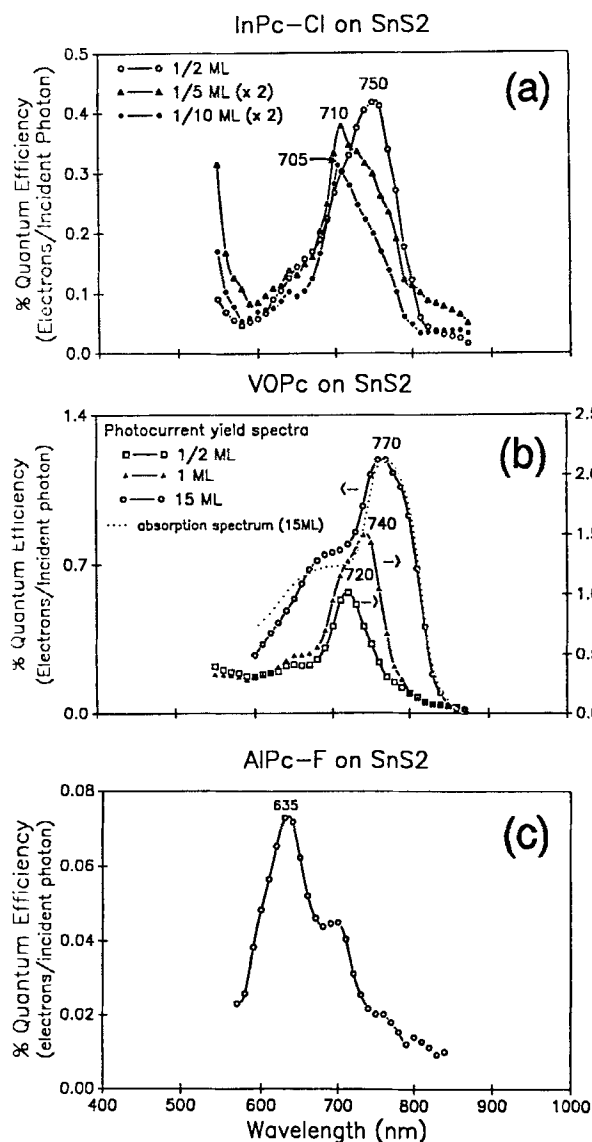


Figure 3 -- InPc-Cl, VOPc and AlPc-F Photocurrent Spectra

spectrum consistent with the onset of formation of at least dimer-like layers (Figure 2a). By the time several multilayers have been formed, the Q-band has shifted to ca. 770 nm, which is within 2 nm of the Q-band maximum reported for epitaxial multilayers of VOPc grown on single crystal KBr.¹¹ Multilayers of VOPc on SnS₂ do not sustain "layer-by-layer" growth as for the first monolayers, when deposited on substrates close to room temperature, but partially ordered films are still possible. Substantially different spectra result, as shown for the photocurrent response and the absorbance spectrum (through a thin slice of the SnS₂ crystal) of an 82 equivalent monolayer VOPc film (Figure 4).

AlPc-F is known to form linear cofacial stacks when deposited at the proper substrate temperatures, and has demonstrated long range ordering over distances of up to hundreds of Pc units.^{6,12} This type of packing leads to a blue shift in the Q-band maximum, relative to the solution monomer spectrum, the extent of which is determined by the number of Pc units in the stack, and their intermolecular spacing. The photocurrent spectra of Figure 3c demonstrate a

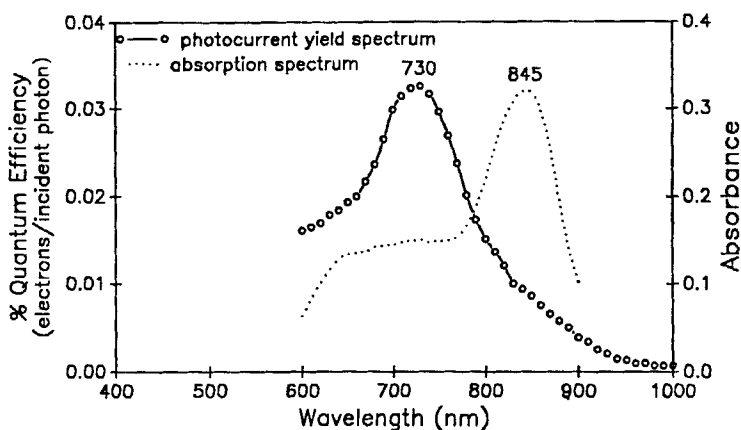


Figure 4 -- Photocurrent, Absorbance Spectra for 82ML VOPc/SnS₂

blue shift to ca. 635 nm for coverages of AlPc-F on the SnS₂ surface of ca. 16ML. This shift is consistent with the formation of a linear cofacial aggregate (Pc rings eclipsed) with average dimensions of at least 6-10 units (see below)^{2,34,35}.

Exciton Splitting in VOPc and AlPc-F Aggregates

The red-shifting in the Q-band spectra of the trivalent metal chloride Pc's has been quantitatively described previously.² The treatment of the VOPc and AlPc-F aggregates follows similar lines of reasoning. Ordered Pc thin films are treated by an extension of the point dipole molecular exciton model of Kasha, originally developed to describe monomolecular lamellar systems.^{34,35} While an extended dipole model is most appropriate for the description of nearest neighbor interactions, the error associated in using a point dipole model has been shown to be minimal for multilayer Pc systems.² The transition dipole strength associated with each Q-band optical transition (3.4×10^{-35} erg \cdot cm³) was determined from the oscillator strength of VOPc (0.46 erg \cdot cm), calculated by integration of the solution monomer absorption band at 14451 cm^{-1} (692 nm). A closest packed monolayer of VOPc, with a square lattice packing geometry (e.g. Figure 1), shows an energy displacement of the Q-band maximum $\epsilon = -4.49M^2/a^3$, where a is the separation distance between molecular centers and M is the transition dipole. Such a calculation leads to a predicted Q-band maximum at ca. 715 nm, close to the observed spectrum at low VOPc coverages. If the second and third VOPc layers are shifted as shown in Figures 2a and 2b, summation of the transition dipole interactions for up to 16 monolayers leads to a movement of the Q-band transition to 769 nm. Such an absorbance peak is seen in both photocurrent and absorbance spectra of MBE-deposited VOPc thin films, and is close to that observed for "Phase III" VOPc grown from melts³⁰ suggesting similarity in their structures.

Two other phases of VOPc are known, at least one of which we believe to form during multilayer deposition, near room temperature, on SnS₂ (Figure 4). Based on the known crystal structure of "Phase-II" VOPc,²⁷⁻³³ summation of the

transition dipole interactions was applied to up to 16 monolayers of this structure with energy displacements given by: $\epsilon = -30.26\text{M}^2/\text{a}^3$ and $-2.64\text{M}^2/\text{a}^3$, for both components of the Q-band. In this structure, the degeneracy of the excited state is removed at the site, and the strong "head-to-tail" coupling of the transition dipoles produces a sizeable splitting -- two bands are expected. Assuming the van der Waals term (D) for the Pc crystal to be $-1,145\text{ cm}^{-1}$ and the solvation energy (S) of VOPc in pyridine to be -452 cm^{-1} the transition energies are predicted at 835 and 730 nm.^{1,2} These predictions agree well with the absorbance spectra of large VOPc coverages on SnS_2 and the transition energy at ca. 835 nm reported by other laboratories.³⁰⁻³³ The presence of two of two absorbance bands of unequal intensity may be related to the removal of excited state degeneracy in this Pc packing structure.

Linear cofacial Pc assemblies, such as the AIPc-F aggregates, produce a parallel coupling of adjacent transition dipoles, leading to Q-band optical transitions in which the higher energy portion of the exciton manifold is preferentially populated, and the band blue shifts from its position in the monomer.^{6,34,35} Using the exciton coupling model, and assuming an eclipsed orientation of the adjacent AIPc-F units, with an interplanar spacing of 3.66\AA , the Q-band maximum for a 16 ML film is predicted to be at 633 nm, within 2 nm of the value observed (Figure 3c).

Photocurrent Spectra -- Quantum Yields

As shown in Figure 5a, the QYAP values for these epitaxial Pc layers exhibit the coverage dependence of photocurrent yield expected from multilayers of dyes.²⁰⁻²⁸ For an absorbance per monolayer ca. 0.013, QYAP is near 50% for lowest coverages of the epitaxial monolayer, and falls with increasing coverage. This is consistent with the hypothesis that only those excited state dyes in intimate contact with the SnS_2 surface undergo exciton dissociation to inject charge into the SnS_2 conduction band. Excitation at other sites create photocurrent only after exciton diffusion, which is competitive with radiative and nonradiative decay pathways.^{22,23} Femtosecond hole-burning spectroscopy studies of these epitaxial monolayers suggests that energy transfer is efficient in these ordered layers.^{11,36,37} Although the QYAP values drop with coverage, this decline is small enough in magnitude to allow quantum yields per incident photon (QYIP) to continue to increase significantly with coverage up to ca. 20-40 monolayers (Figure 5b). From these data it appears that exciton transport is reasonably efficient up to Pc film thicknesses of ca. $80\text{-}160\text{\AA}$, which is consistent with reported exciton diffusion lengths in such materials.^{38,39} As expected, the QYAP values at comparable Pc coverages scale linearly with the oscillator strength of the monomer in the order $\text{GaPc-Cl} > \text{AIPc-Cl} > \text{InPc-Cl}$. The QYAP and QYIP values are also strongly dependent upon the energy of the excited state achievable in the Pc aggregate. As shown in Figure 4, the VOPc aggregates formed at higher coverages on the SnS_2 surface do not produce photocurrent proportional to the absorbance spectral response. The lowest energy portion of the exciton manifold is apparently not capable of injection of charge at the SnS_2 conduction band energy.

Estimates have been made of the positions of the SnS_2 conduction and valence band edge on an electrochemical potential scale placing $E_{\text{CB}} = -0.42$ V and $E_{\text{VB}} = +1.80$ V vs. Ag/AgCl .¹⁹ Estimates of the first oxidation (electrochemical studies⁴⁰), or first ionization potentials (UPS studies⁴¹), allow an estimate of the approximate position of the ground states of these Pc dyes with respect to the same Ag/AgCl reference electrode. The ground states of VOPc, InPc-Cl, GaPc-Cl, and AlPc-Cl, are placed respectively at +1.08, +1.15, +1.18, and +1.23 V vs. Ag/AgCl . Consequently, the lower energy optical transitions, at wavelengths longer than ca. 825, 790, 775, and 750 nm for VOPc, InPc-Cl, GaPc-Cl, and AlPc-Cl respectively, are not likely to produce a sufficiently energetic intermediate to inject electrons into SnS_2 , thus leading to the differences between absorbance and photocurrent spectra seen in data like that of Figure 4.

The QYAP and QYIP values for AlPc-F ultrathin films on SnS_2 are uniformly lower at all coverages than seen for the other trivalent and tetravalent metal Pc's (Figure 3c). In these linear cofacial assemblies, relaxation of the excited state to the lowest part of the singlet manifold is less probable than for the staggered aggregates, and decay of this excited state through intersystem crossing and triplet formation is likely to be enhanced.^{34,35} Charge injection from such triplet states into the SnS_2 conduction band is not expected to be as efficient as injection from the lowest singlet states in the other Pc aggregates, especially if their energies are below those of the lowest energy singlet states referred to above.¹⁹

The fact that the quantum values for sensitization from AlPc-F aggregates are at least an order of magnitude lower versus the other trivalent metal Pc chlorides (including AlPc-Cl aggregates) tends to confirm the difficulty in charge injection from such states.

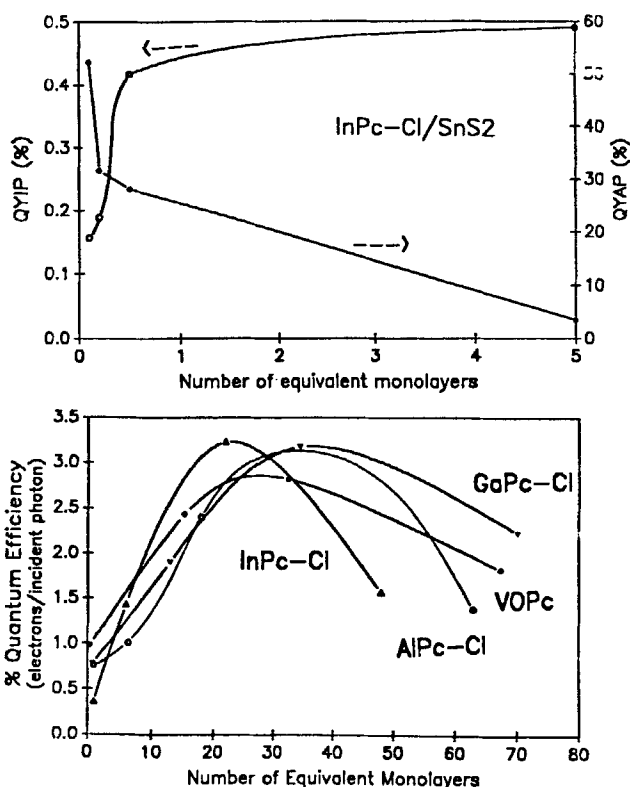


Figure 5 -- QYAP, QYIP vs. Γ_{Pc}

These studies are also significant in their relationship to characterization of SnS_2 dye sensitization by liquid crystalline, (LC-Pc) assemblies, produced from phthalocyanines modified with various hydrocarbon side chains.⁴³ In those studies it has been observed that the formation of linear cofacial multilayer assemblies can be distinguished from closest packed, flat lying monolayers of the LC-Pc, by virtue of their photocurrent action spectra. The first monolayer of LC-Pc adsorbed to the photoelectrode surface sensitizes the SnS_2 response with the same efficiencies as seen for the MBE deposited Pc's, and produces Q-band spectra of the same shape and position as seen for the best quality epitaxial dyes thus reported. Photoelectrochemical studies will continue to be an important spectroscopic tool in the characterization of ultrathin films of this new class of materials.

Conclusions

For vacuum compatible dyes it is now possible to create a wide range of ordered structures by MBE approaches. This work now is being extended to other substrates which minimize the number of equivalent domains formed in the first few monolayers and/or which have particular electronic or optoelectronic interest (e.g. $\text{Cu}(100)$, $\text{TiO}_2(001)$, $\text{Si}(111)\text{-H}$). Where applicable, dye sensitization photoelectrochemical processes will play an important role in the characterization of the initial stages of nucleation and growth of these thin films. Multilayers of phthalocyanines and perylenes (and other weak acceptors such as the fullerenes), are of special interest in heterojunction formation, especially in those cases where each dye layer exhibits long range order. Photoelectrochemical characterization of such structures can be utilized to isolate the most photoactive interfaces, and to characterize the distance over which exciton dissociation events occur near the interface between two dissimilar dye layers.⁴² For these materials, and those of interest in photonics, it is now important to test whether long range order can impart unique optical and/or electrical properties to ultrathin dye layers where two and three-dimensional chromophore interaction is maximized.

Acknowledgments -- This research was supported by grants from NSF (Chemistry and Small Grants for Exploratory Research), AFOSR, and the Materials Characterization Program, State of Arizona.

References

1. L.-K. Chau, C. Arbour, G.E. Collins, K.W. Nebesny, P.A. Lee, E.D. England, N.R. Armstrong, B.A. Parkinson, *J. Phys. Chem.*, **97**, 2690 (1993).
2. L.-K. Chau, C.E. England, S.-Y. Chen, N.R. Armstrong, *J. Phys. Chem.*, **97**, 2699, (1993).
3. G.E. Collins, K.W. Nebesny, C.D. England, L.-K. Chau, P.A. Lee, B.A. Parkinson, and N.R. Armstrong, *J. Vac. Sci. Technol. A*, **10**, 2902 (1992).
4. K.W. Nebesny, G.E. Collins, P.A. Lee, L.-K. Chau, J.L. Danziger, E. Osburn, and N.R. Armstrong, *Chem. Mater.*, **3**, 829 (1991).
5. P.E. Burrows, M. Hara, and H. Sasabe, *Mol. Cryst. Liq. Cryst. Sci. Technol. B*, **2**, 193 (1992);
6. A.J. Dann, H. Hoshi, and Y. Maruyama, *J. Appl. Phys.*, **67**, 1371 (1990).
7. H. Tada, K. Saiki, and A. Koma, *Jap. J. Appl. Phys.*, **30**, L306 (1991).
8. H. Tada, T. Kawaguchi, and A. Koma, *Appl. Phys. Lett.*, **61**, 2021 (1992).
9. H. Tada, K. Saiki, and A. Koma, *Surf. Sci.*, **268**, 387 (1992).
10. M. Hosoda, T. Wada, A. Yamada, A.F. Garito, and H. Sasabe, *Jap. J. Appl. Phys.*, **30**, L1486 (1991).
11. A. Terasaki, M. Hosoda, T. Wada, H. Tada, A. Koma, A. Yamada, H. Sasabe, A.F. Garito, and T. Kobayashi, *J. Phys. Chem.*, **96**, 10534 (1992).
12. J.R. Fryer, *Mol. Cryst. Liq. Cryst.*, **137**, 49 (1986).
13. H. Yanagi, S. Douko, Y. Ueda, M. Ashida, and D. Wöhrle, *J. Phys. Chem.*, **96**, 1366 (1992).
14. M. Möbus, N. Karl and T. Kobayashi, *J. Cryst. Growth*, **116**, 495 (1992).
15. H. Yanagi, M. Ashida, J. Elba, and D. Wöhrle, *J. Phys. Chem.*, **94**, 7056 (1990).
16. A. Manivannan, L.A. Nagahara, K. Hashimoto and A. Fujishima, *Langmuir*, **9**, 771 (1993).
17. M. Hara, H. Sasabe, A. Yamada, and A.F. Garito, *Jap. J. Appl. Phys.*, **28**, L306 (1989).
18. C.D. England, G.E. Collins, T. Schuerlein, N.R. Armstrong, in preparation.
19. B.A. Parkinson, *Langmuir*, **4**, 967 (1988).
20. B.A. Parkinson, and M.T. Spitler, *Electrochim. Acta*, **37**, 943 (1992).
21. L.M. Natoli, M.A. Ryan, and M.T. Spitler, *J. Phys. Chem.*, **89**, 1448 (1985).
22. M. van der Auweraer, and F. Willig, *Isr. J. Chem.*, **25**, 274 (1985).
23. H. Gerischer and F. Willig, in *Topics in Current Chemistry*, Vol. 61, Springer-Verlag: New York, 1976, p. 31.
24. M.A. Ryan and M.T. Spitler, *J. Imaging Sci.*, **183**, 46 (1989).
25. T. Tani, T. Suzumoto, K. Kemnitz, and K. Yoshihara, *J. Phys. Chem.*, **96**, 2778 (1992).
26. W. West, and B.H. Carroll, *J. Chem. Phys.*, **19**, 417 (1951).
27. K.J. Wynne, *Inorg. Chem.*, **23**, 4658 (1984).

28. W. Hiller, J. Strähle, W. Kobel, and M. Hanack, *Z. Krist.*, **159**, 173 (1982).
29. R.F. Ziolo, C.H. Griffiths, and J.M. Troup, *J. Chem. Soc. Dalton Trans.*, 2300 (1980).
30. C.H. Griffiths, M.S. Walker, and P. Goldstein, *Mol. Cryst. Liq. Cryst.*, **33**, 149 (1976).
31. T.-H. Huang and J.H. Sharp, *Chem. Phys.*, **65**, 205 (1982).
32. R. Aroca and L.O. Loutfy, *Spectrochim. Acta*, **39A**, 847 (1983).
33. T. Klofta, C. Linkous, and N.R. Armstrong, *J. Electroanal. Chem.*, **185**, 73 (1985).
34. M. Kasha, H.R. Rawles, M.A. El-Bayoumi, *Pure Appl. Chem.*, **11**, 371 (1965).
35. R.M. Hochstrasser and M. Kasha, *Photochem. Photobiol.*, **3**, 317 (1964).
36. V.S. Williams, S. Mazumdar, Z.Z. Ho, N.R. Armstrong, and N. Peyghambarian, *J. Phys. Chem.* **96**, 4500 (1992).
37. V. Williams, Sandalphon, N.R. Armstrong, N. Peyghambarian, S. Mazumdar, manuscript in preparation.
38. R.O. Loutfy, J.H. Sharp, C.K. Hsiao, and R. Ho, *J. Appl. Phys.*, **52**, 5218 (1981).
39. B. Blanzat, C. Barthou, N. Tercier, J.-J. André, and J. Simon, *J. Am. Chem. Soc.*, **109**, 6193 (1987).
40. A.B.P. Lever, S. Licoccia, K. Magnell, P.C. Minor, and B.S. Ramaswamy, In *"Electrochemical and Spectrochemical Studies of Biological Redox Components"*, K.M. Kadish, Ed., Adv. Chem. Series 201, ACS: Washington, D.C., 1982, Chapter 11.
41. J. Danziger, J.-P. Dodelet, P. Lee, K.W. Nebesny, and N. R. Armstrong, *Chem. Mater.*, **3**, 821 (1991).
42. L.-K. Chau, E.J. Osburn, N.R. Armstrong and D.F. O'Brien, *Langmuir*, in press.